Numerical calculation of the magnetodielectric anisotropy effect in magnetic fluids

J. Shobaki
Department of Physics, Yarmouk University, Irbid, Jordan

S. Musameh
An-Najah University, Nablus, West Bank

F. Rawwagah
Center for Theoretical and Applied Physics, Yarmouk University, Irbid, Jordan

N. A. Yusuf
Department of Physics, Yarmouk University, Irbid, Jordan

(Received 17 November 1995; revised manuscript received 25 July 1996)

The magnetodielectric anisotropy effect in Fe_3O_4 particle magnetic fluid has been numerically calculated. Our results, in agreement with previously reported results, show that the dielectric constant in the direction parallel to the field increases with the applied field, while that normal to the field decreases. The results also, in agreement with previous results, show that the dielectric constant in the field direction increases with temperature above a given temperature T_s reaching a maximum at T_m then decreases for higher temperatures; while in the direction normal to the field it decreases with temperature for temperatures above T_s reaching a minimum at T_m then increases for higher temperatures. Furthermore, our results show the important role that dimensionality plays on the magnetodielectric anisotropy effect. [S0163-1829(96)03542-4]

I. INTRODUCTION

Magnetodielectric effect in magnetic fluids have been investigated by many workers[1–12] both experimentally and theoretically. The experimental investigations were based on impedance measurement techniques where the magnetic fluid is placed in a capacitor. Measurements of the impedance parameters such as the modulus and phase are carried out using a bridge or an RLC meter.[1–8] It is known that impedance measurement techniques suffer some serious disadvantages such as electrode effects, parasitic impedances, skin depth, and accuracy related problems. Very recently Yusuf *et al.*[9] have determined the magnetodielectric effect from magnetooptical measurements where the disadvantages suffered by conventional impedance measurement techniques are avoided.

On the theoretical side, Monte Carlo simulations were used to calculate the magnetodielectric anisotropy effect.[10–12]

In most of the previous works the magnetodielectric anisotropy factor which is defined as

$$g(H,\omega)=\frac{\varepsilon_{\parallel(H,\omega)}-\varepsilon_{0(0,\omega)}}{\varepsilon_{0(0,\omega)}-\varepsilon_{\perp(H,\omega)}},$$

was either 1 (Refs. 3, 7, and 9) or 2.[2,6,10,23] In this work the dielectric constant, $\varepsilon_{\parallel}$ parallel to the applied field and $\varepsilon_{\perp}$ in a direction perpendicular to the field are numerically calculated for two cases, one for a two-dimensional (2D) sample and the other for a three-dimensional (3D) sample. In our calculations it is assumed that the dielectric constant at a given wavelength in a magnetic fluid is proportional to the average projection length of the particles in the fluid. Our results show that $g(H,\omega)$ is 1 for the 2D case and is two for the 3D case. It is worth mentioning that calculations of the optical anisotropy in magnetic fluids have been carried out using similar procedure.[24]

II. THEORETICAL BACKGROUND

The dielectric constant of a magnetic fluid in the absence of an external magnetic field exhibits no anisotropy due to the random orientation of the particles. Therefore, the dielectric constant seen by light with different states of polarization is the same. However, when a magnetic field is applied, orientation of particles and field-induced chain formation in the field direction take place leading to two different average lengths $l_{\parallel}$ in the field direction and $l_{\perp}$ perpendicular to the field; consequently the dielectric constant will exhibit some degree of anisotropy.

The magnetic moments of the colloidal particles in a magnetic fluid reach thermal equilibrium via two distinct mechanisms. The first is the Néel mechanism with a relaxation time given by[12]

$$\tau_N=[M_{sB}/2\alpha\gamma K][k_BT/KV]^{1/2}\exp[KV/k_BT], \qquad (1)$$

where α is an attenuation factor, γ is the gyromagnetic ratio, K is the effective anisotropy constant, V is the magnetic volume of the particle, and T is the absolute temperature. The second mechanism is the Brownian mechanism with a relaxation time given by[12]

$$\tau_B=3\eta V's/k_BT, \qquad (2)$$

where η is the viscosity of the magnetic fluid, V' is the hydrodynamic volume of the particle, and s is a geometrical factor ($s=1$ for spherical particles).

The dominant relaxation mechanism is the one with the shorter relaxation time. The Néel relaxation time given by Eq. (1) grows exponentially with the magnetic volume, therefore, only small particles may relax via the Néel relaxation mechanism. Due to the presence of a particle size distribution in the sample a volume at which $\tau_N = \tau_B$ exists. This volume is known as the Shliomis volume, V_s.[13,14]

The magnetodielectric anisotropy effect in magnetic fluid is a consequence of the orientation of single particles and clusters in the fluid; and to the field-induced chain formation. This requires that particles relax physically via the Brownian relaxation mechanism.

Only particles with $V > V_s$ will relax via the Brownian mechanism, thus contributing to the magnetodielectric anisotropy effect. It is, therefore, necessary to determine the Shliomis volume V_s. This is accomplished by equating the two relaxation times and assuming $V = V'$ yielding the following transcendental relation:

$$q^{-3/2}\exp(q) = 6\,\eta\alpha\gamma M_{sb}^{-1}, \tag{3}$$

where $q = (KV_s)/(k_BT)$. The relation in Eq. (3) is numerically solved for the Shliomis volume V_s.

The orientation function $\phi(p,q)$ for a uniaxial single-domain particle suspended in a nonmagnetic liquid carrier under the application of an external magnetic field was treated by Hartmann and Mende[15,16] and Scholten[17,18] and is given by

$$\phi(p,q) = \xi(q) f(p), \tag{4}$$

where $\xi(q)$ represents the coupling between the magnetic moment of the particle and its easy axis and is usually expressed as

$$\xi(q) = \frac{3}{4q}\left[\frac{q^{1/2}\exp(q) - I(q)}{I(q)}\right] - 1/2, \tag{5}$$

where

$$I(q) = \int_0^{q^{1/2}} \exp(x^2)\,dx. \tag{6}$$

The function $f(p)$ is given by

$$f(p) = [1 - (3/p)L(p)], \tag{7}$$

where $L(P)$ is the Langevin function, and $p = (\mu_0 M_{sB} V H/k_B T)$.

For an ellipsoidal particle with a major axis a and a minor axis b, the average projection lengths $l_\parallel$ and $l_\perp$ for a two-dimensional system are expressed as

$$l_\parallel = a[1 + \phi(p,q)] + b[1 - \phi(p,q)], \tag{8}$$

and

$$l_\perp = a[1 - \phi(p,q)] + b[1 + \phi(p,q)]. \tag{9}$$

These two equations ensure the boundary condition that $l_\parallel$ and $l_\perp$ are the same and equal to $(a+b)$ at zero field where $\phi(p,q) = 0$; and that $l_\parallel = 2a$ and $l_\perp = 2b$ at very high fields where $\phi(p,q) = 1$.

For a three-dimensional system with a field applied in the z direction the average projection lengths are expressed as

$$l_z = a[1 + \phi(p,q)] + b[1 - \phi(p,q)], \tag{10}$$

$$l_x = a[1 - \phi(p,q)/2] + b[1 + \phi(p,q)/2], \tag{11}$$

and

$$l_y = a[1 - \phi(p,q)/2] + b[1 + \phi(p,q)/2]. \tag{12}$$

Therefore, $l_\parallel$ and $l_\perp$ are given by

$$l_\parallel = a[1 + \phi(p,q)] + b[1 - \phi(p,q)], \tag{13}$$

and

$$l_\perp = a[1 - \phi(p,q)/2] + b[1 + \phi(p,q)/2]. \tag{14}$$

Taking into consideration the particle size distribution, the total projection lengths, for a 2D system will be given by

$$l_{\parallel t} = \int_{V_{\min}}^{V_s} (a+b)F(v)\,dv + \int_{V_s}^{V_{\max}} \{a[1 + \phi(p,q)] + b[1 - \phi(p,q)]\}F(v)\,dv \tag{15}$$

and

$$l_{\perp t} = \int_{V_{\min}}^{V_s} (a+b)F(v)\,dv + \int_{V_s}^{V_{\max}} \{a[1 - \phi(p,q)] + b[1 + \phi(p,q)]\}F(v)\,dv, \tag{16}$$

and for a 3D system they are given by

$$l_{\parallel t} = \int_{V_{\min}}^{V_s} (a+b)F(v)\,dv + \int_{V_s}^{V_{\max}} \{a[1 + \phi(p,q)] + b[1 - \phi(p,q)]\}F(v)\,dv \tag{17}$$

and

$$l_{\perp t} = \int_{V_{\min}}^{V_s} (a+b)F(v)\,dv + \int_{V_s}^{V_{\max}} \{a[1 - \phi(p,q)/2] + b[1 + \phi(p,q)/2]\}F(v)\,dv, \tag{18}$$

where $V_{\min}$ and $V_{\max}$ are the minimum and maximum volumes in the distribution, respectively, and V_s is the Shliomis volume.

Since the viscosity plays an important role in determining the Shliomis volume V_s, we review the basic relevant relations describing the variation of viscosity with temperature, field, and concentration. For low concentration of spherically shaped particles, the viscosity variation with concentration is presented by the Einstein formula:[11]

$$\eta = \eta_0[1 + 2.5\varepsilon], \tag{19}$$

where η_0 is the viscosity of the liquid carrier and ε is the volumic fraction of the magnetic particles in the fluid. The variation of viscosity with the field is given by[17]

$$\eta = \eta_0\left\{1 + \frac{\epsilon}{2}\left[5 + 3\left(\frac{p - \tanh p}{p + \tanh p}\right)\sin^2\vartheta\right]\right\}, \tag{20}$$

where ϑ is the angle between the magnetic field and the local angular velocity of the liquid.

The variation of viscosity with temperature is expressed as[19–21]

$$\eta = \eta_0 \exp\left[\frac{A}{T-T_0}\right], \tag{21}$$

where A is a characteristic positive constant and T_0 is a temperature below the melting temperature of the fluid. Shliomis and Stepanov[22] have experimentally determined the constants which appear in Eq. (21) for Fe_3O_4 particle magnetic fluid with kerosene as a liquid carrier, (i.e., $\eta_0 = 5.77\times10^{-3}$, $A = 396$ K, and $T_0 = 162$ K).

III. METHOD OF CALCULATION

The total average length $l_\parallel$ and $l_\perp$ were calculated for magnetic fluids with magnetic particles of different uniform sizes, log-normal, and normal size distributions. The first step in the calculation is determining the Shliomis volume V_s at a given temperature and for a given applied field by numerically solving Eq. (3). For particles with a uniform size V the Shliomis volume at a given temperature and for a given applied field V_s is compared to the size of the particles, and if $V_s > V$, both $l_\parallel$ and $l_\perp$ are set equal to $(a+b)$. However if $V_s \leqslant V$, the parameter q is calculated and the integral $I(q)$ given in Eq. (6) is numerically evaluated, and consequently the function $\xi(q)$ is evaluated. Moreover, for a given measuring field H and a given temperature, the parameter p is calculated for the volume V, and consequently the function $f(p)$ given in Eq. (7) is evaluated. Therefore the orientation function $\phi\ (p,q)$ is evaluated, and the average projection lengths $l_{\parallel t}$ and $l_{\perp t}$ are then obtained from Eqs. (8) and (9) for the two-dimensional system, and from Eqs. (13) and (14) for the three-dimensional system. By multiplying the average projection lengths by a constant (for a given wavelength), which is proportional to the concentration, the relative dielectric constant is obtained. Dividing these quantities by their corresponding values at zero fields [ε_0 which is equal to $(a+b)$ multiplied by the same constant], yields $(\varepsilon_\parallel/\varepsilon_0)$ and $(\varepsilon_\perp/\varepsilon_0)$. These calculations are repeated for different temperatures and different applied magnetic fields for different single volumes. The axial ratio (a/b) used in these calculations ranged from 1.0 to 2.0.

For a particle size distribution the Shliomis volume at a given temperature and at a given applied field V_s is compared to the distribution and if $V_s > V_{\max}$ then the average lengths $l_\parallel$ and $l_\perp$ are taken equal to that when the applied field is zero l_0, where l_0 is given by

$$l_0 = \int_{V_{\min}}^{V_{\max}} (a+b) F(v)\, dv. \tag{22}$$

However if $V_s \leqslant V_{\max}$, then particles with volumes $V_s \leqslant V \leqslant V_{\max}$ will orient with the field and the values of $l_\parallel$ and $l_\perp$ are given by Eqs. (8) and (9) for the 2D system, and Eqs. (13) and (14) for the 3D system. The range of volumes between $V_{\min}$ and $V_{\max}$ is divided into a number of narrow slices, and for each volume in this range the values $l_\parallel$ and $l_\perp$ are evaluated with the same procedure used in the case of particles with uniform sizes. The total average lengths at a given temperature and a given applied field is then obtained by numerically integrating over the volume range from $V_{\min}$ to $V_{\max}$ using Eqs. (15) and (16) for the 2D system and Eqs. (17) and (18) for the 3D system. Changing the temperature or the applied field will change the Shliomis volume and consequently the range of volumes for which particles will orient with the field will change. The relative dielectric constants $(\varepsilon_\parallel/\varepsilon_0)$ and $(\varepsilon_\perp/\varepsilon_0)$ are then calculated from $(\varepsilon_\parallel/\varepsilon_0 = l_{\parallel t}/l_0)$ and $(\varepsilon_\perp/\varepsilon_0 = l_{\perp t}/l_0)$.

TABLE I. The values of the general constants used in the calculations.

Effective anisotropy constant	$K = 5\times10^4$ J/m^3
Attenuation factor	$\alpha = 1\times10^{-2}$
Gyromagnetic ratio	$\gamma = 1.7\times10^7$ s^{-1} G^{-1}
Saturation magnetization	$M_s = 485\times10^3$ A/m
Constant A in Eq. (13)	$= 396$ K

The effect of the applied magnetic field on the anisotropy energy, i.e., replacing KV by $KV\,[1+(H/H_K)^2]$, where H_K is the anisotropy $(M_{sB}/2K)$ field has been introduced in the Néel relaxation time given in Eq. (1). Furthermore, the effect of applied field on viscosity is taken into consideration by using Eq. (20). However, the average value (1/2) of $\sin^2\vartheta$ in Eq. (20) is used in the calculations of the average projection lengths and in the relative dielectric constants.

The effect of concentration on the calculation is introduced in the variation of viscosity with concentration, and in the variation of viscosity with temperature, Eq. (21), by slightly changing the value of T_0. The values of the general constants used in the calculations are listed in Table I.

The reduced dielectric constant was calculated for uniform size Fe_3O_4 magnetic particles dispersed in kerosene, with volumic fraction ε equal to 0.05. Four different volumes of the particles were used ($V = 6, 8, 10, 12, 14\times10^{-25}$ m^3). The initial viscosity $\eta_0 = 5.77\times10^{-3}$ Pa and $T_0 = 165$ K were used in the calculations.

Furthermore, the reduced dielectric constant for Fe_3O_4 particle magnetic fluid with kerosene as a liquid carrier and volumic fraction $\varepsilon = 0.05$ was calculated for normal and log-normal distributions with particle average volume of 8×10^{-25} m^3 and a standard deviation of 1×10^{-25} m^3 and 0.15, respectively. The effect of the liquid carrier on the magnetodielectric effect is investigated by changing the initial viscosity and changing the parameter T_0.

IV. RESULTS

The magnetodielectric anisotropy effect for uniform size ($V = 8\times10^{-25}$ m^3) Fe_3O_4 particle magnetic fluid (different axial ratios) with kerosene as a liquid carrier at a temperature $T = 300$ K versus magnetic field is presented in Figs. 1(a) and 1(b) for the 2D and 3D systems, respectively. The results in the figure show that both $(\varepsilon_\parallel/\varepsilon_0)$ and $(\varepsilon_\perp/\varepsilon_0)$ starts practically from 1.0 at very low fields and that $(\varepsilon_\parallel/\varepsilon_0)$ increases rapidly for intermediate fields and tends to saturate at high fields; while $(\varepsilon_\perp/\varepsilon_0)$ decreases rapidly for intermediate fields and levels off at high fields. The rate of increase for $(\varepsilon_\parallel/\varepsilon_0)$ and the rate of decrease for $(\varepsilon_\perp/\varepsilon_0)$ are dependent on the axial ratio (a/b) being the highest for the highest axial ratio. The highest value of $(\varepsilon_\parallel/\varepsilon_0)$ and the lowest value of $(\varepsilon_\perp/\varepsilon_0)$ occur for the highest axial ratio. The results also show that for an

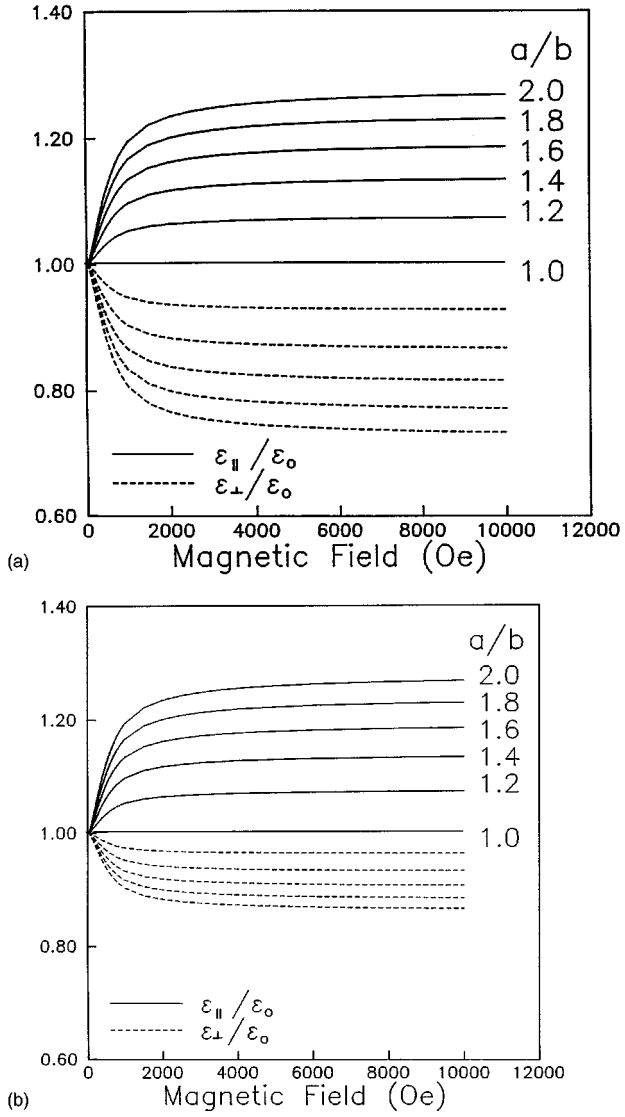

FIG. 1. The magnetodielectric anisotropy effect for particles with single volume $V=8\times10^{-25}$ m^3 and different axial ratios; (a) for a 2D sample, (b) for a 3D sample.

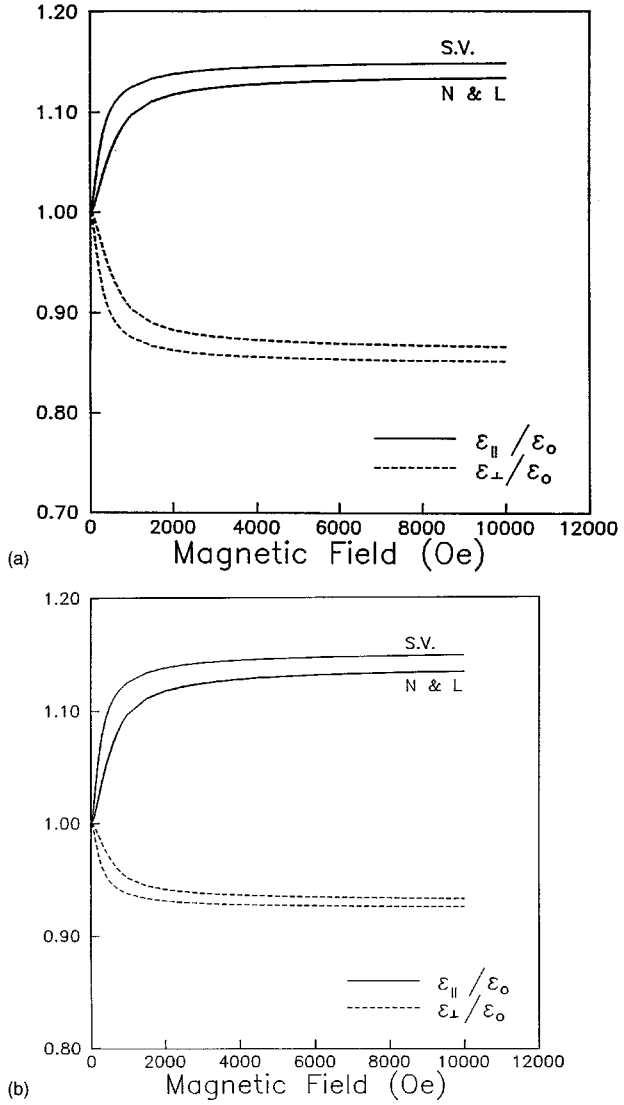

FIG. 2. The magnetodielectric anisotropy effect for single, normal, and log-normal size distribution with the same average volumes; (a) for a 2D sample, (b) for a 3D sample.

axial ratio of 1.0, i.e., spherical particles, the magnetodielectric effect is absent. Furthermore, the results show that $g(H,\omega)=1$ for the 2D system and it is equal to 2 for the 3D system.

The magnetodielectric anisotropy effect for a magnetic fluid with ($\varepsilon=0.05$) at temperature $T=300$ K for single volume, normal distribution and log-normal distribution are presented in Figs. 2(a) and 2(b) For the 2D and 3D cases, respectively. For both cases the average volume for the two distributions is taken equal to the single volume ($V=8\times10^{-25}$ m^3) but the standard deviation is taken 1×10^{-25} and 0.15, for the normal and log-normal distributions, respectively. For the three size distributions the axial ratio is 1.2. The results show that the magnetodielectric anisotropy effect is the same for the two distributions and is slightly different for the single volume case. However, although increasing the axial ratio leaves the similarity between the two distributions unchanged, the difference between them and the single volume case is further reduced. Furthermore the results in Fig. 2 show that $g(H,\omega)=1$ for the 2D sample and is equal to 2 for the 3D sample.

The magnetodielectric anisotropy effect in a magnetic fluid for normal size distribution with average volumes of 6, 8, 10, 12, and 14×10^{-25} m^3, axial ratio $(a/b)=1.2$ and a standard deviation $\sigma=1\times10^{-25}$ m^3 are presented in Figs. 3(a) and 3(b) for the 2D and 3D cases, respectively. The results in the figure show that the higher the average volume is, the higher the magnetodielectric anisotropy effect is. Also the results in the figure show that when the average volume is small the magnetodielectric anisotropy effect does not appear until the field is appreciable. Furthermore increasing the axial ratio increases the difference in the effect for the different volumes. Furthermore, again the results in Fig. 3 show that $g(H,\omega)=1$ for the 2D sample and is equal to 2 for the 3D sample.

In Fig. 4 the Shliomis volume V_s is presented as a function of temperature for a magnetic fluid with volumic fraction $\varepsilon=0.05$ and for an applied magnetic field $H=500$ Oe. The magnetodielectric anisotropy effect versus temperature in a magnetic fluid with uniform, normal, and log-

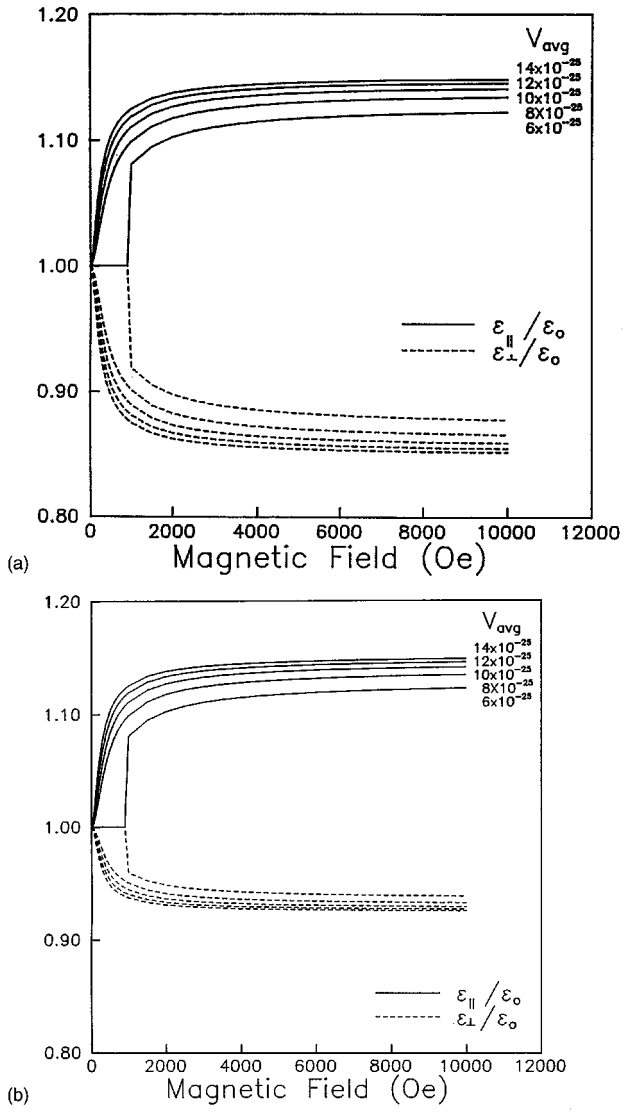

FIG. 3. The magnetodielectric anisotropy effect for normal size distribution particles with the same axial ratio and standard deviation but with different average volumes; (a) for a 2D sample, (b) for a 3D sample.

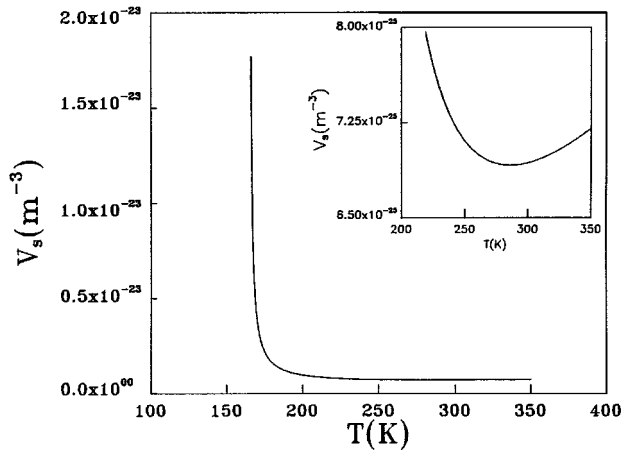

FIG. 4. The Shliomis volume V_s versus temperature at a measuring field $H=500$ Oe.

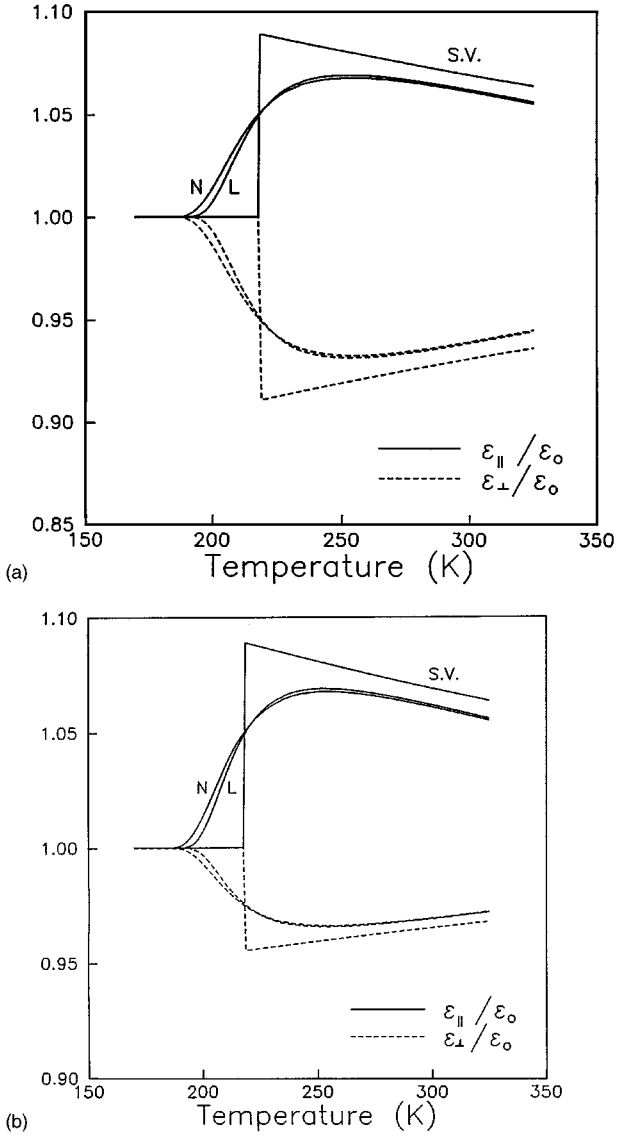

FIG. 5. The magnetodielectric anisotropy effect versus temperature for single, normal, and log-normal size distribution; (a) for a 2D sample, (b) for a 3D sample.

normal size distributions measured at $H=500$ Oe is presented in Figs. 5(a) and 5(b) for the 2D and 3D cases, respectively. The average volume for both distributions is equal to the single volume $V=8\times10^{-25}$ m^3 and the axial ratio for the three cases is 1.6. The standard deviation is 1×10^{-25} and 0.15 for the normal and log-normal distributions, respectively. Although the results in the figure show that the magnetodielectric anisotropy effect is absent below a given temperature, this temperature is different for the different size distributions, being the lowest for the normal distribution. Furthermore the results also show that the increase to the maximum of $(\varepsilon_{\|}/\varepsilon_0)$ and the decrease to the minimum of $(\varepsilon_{\perp}/\varepsilon_0)$ is gradual in the case of the size distributions, while it is abrupt in the case of the single size. The results also show that the magnetodielectric anisotropy effect for the normal or a log-normal size distribution are practically imposed but still deviate from those for a single volume. Again the results in the figure show that $g(H,\omega)=1$ for the 2D sample and is equal to 2 for the 3D sample.

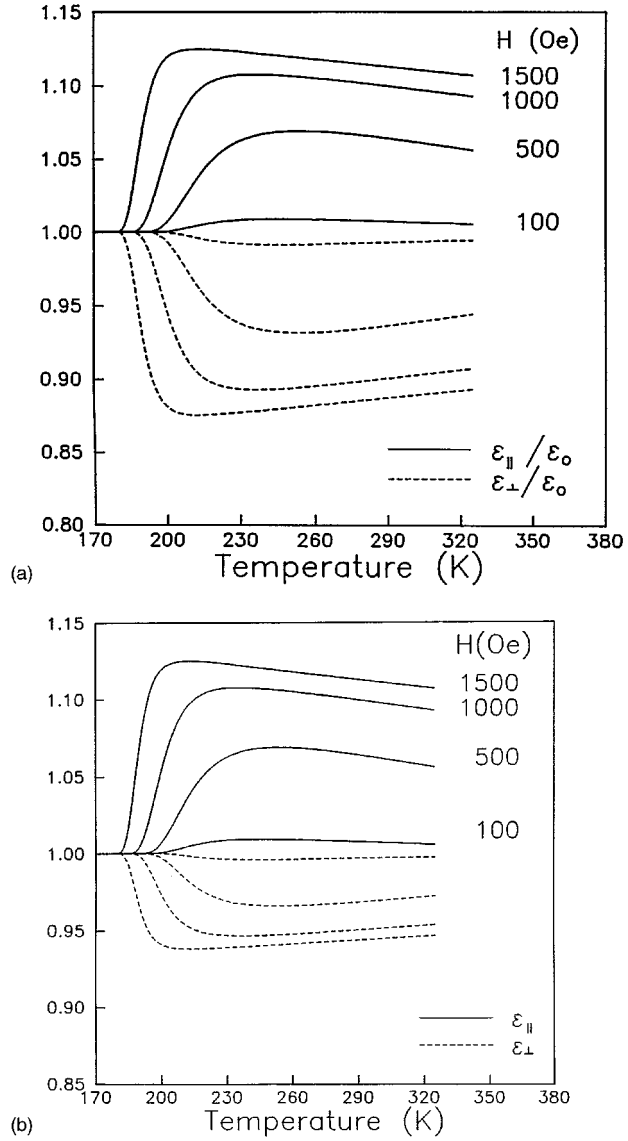

FIG. 6. The magnetodielectric anisotropy effect for normal distribution versus temperature for different applied measuring fields; (a) for a 2D sample, (b) for a 3D sample.

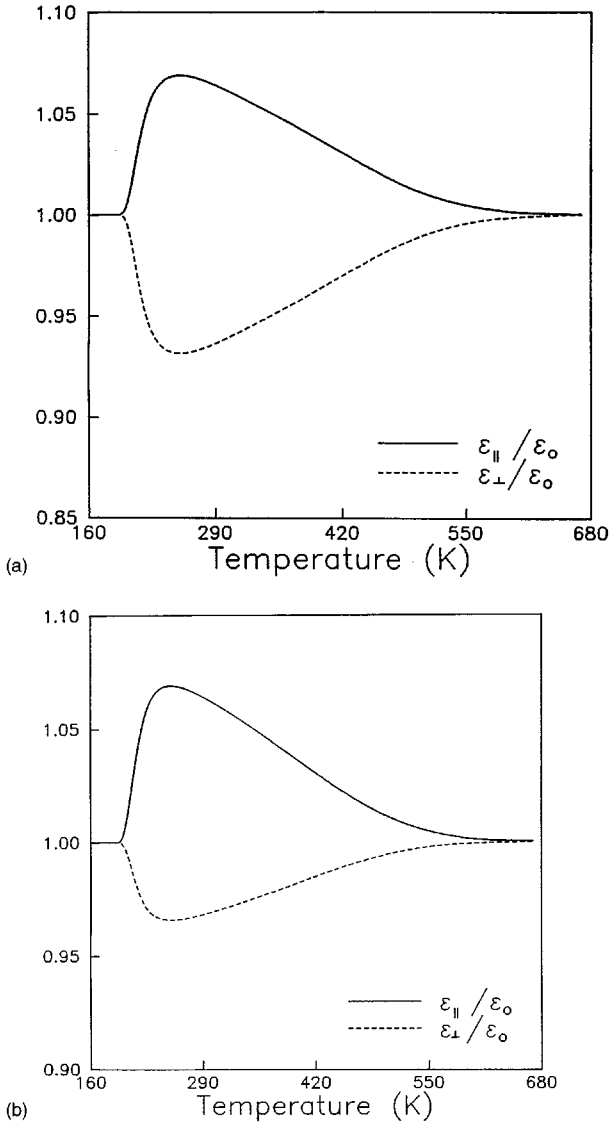

FIG. 7. The magnetodielectric anisotropy effect versus temperature for normal size distribution; (a) for a 2D sample, (b) for a 3D sample.

The magnetodielectric anisotropy effect for a magnetic fluid, (ε=0.05) with normal size distributions of an average volume=8×10^{-25} m^3 and standard deviation $\sigma=1\times10^{-25}$ m^3 and an axial ratio of 1.2 at different applied magnetic fields versus temperature is presented in Figs. 6(a) and 6(b) for the 2D and 3D cases, respectively. The results in the figure show that the magnetodielectric anisotropy effect is absent below a given temperature then gradually increases to a maximum at T_m then decreases for higher temperatures. Again $g(H,\omega)=1$ for the 2D sample and is equal to 2 for the 3D sample.

Increasing the temperature to a high enough value resulted in $(\varepsilon_{\parallel}/\varepsilon_0)$ and $(\varepsilon_{\perp}/\varepsilon_0)$ converging towards each other as is seen in Figs. 7(a) and 7(b). The temperatures at which the magnetodielectric anisotropy effect appears and at which it reaches an optimum are field dependent being the lowest for the highest field. Furthermore, changing the axial ratio, changes the magnitude of the effect, but does not change the temperature at which the effect appears, as can be seen in Figs. 8(a) and 8(b). The effect of the average volume on the temperature variation of the magnetodielectric anisotropy effect is presented in Figs. 9(a) and 9(b). The results in the figure show that the higher the average volume is the higher the effect is, and more importantly the lower the temperature at which optimum conditions in the effect occurs.

The effect of viscosity on the magnetodielectric anisotropy effect is presented in Figs. 10(a) and 10(b). The results show that the higher the viscosity is the lower the effect is and the higher the temperature at which the maximum in $\varepsilon_{\parallel}/\varepsilon_0$ and the minimum in $\varepsilon_{\perp}/\varepsilon_0$ occurs is.

V. DISCUSSION

The magnetodielectric anisotropy effect presented in Fig. 1(a) which is calculated for a 2D sample is qualitatively similar to the experimental results reported by Cotae,[3] Yusuf *et al.*,[9] and those reported by Espurz, Alameda, and Espurz-Nieto.[7] The results for the 3D sample presented in

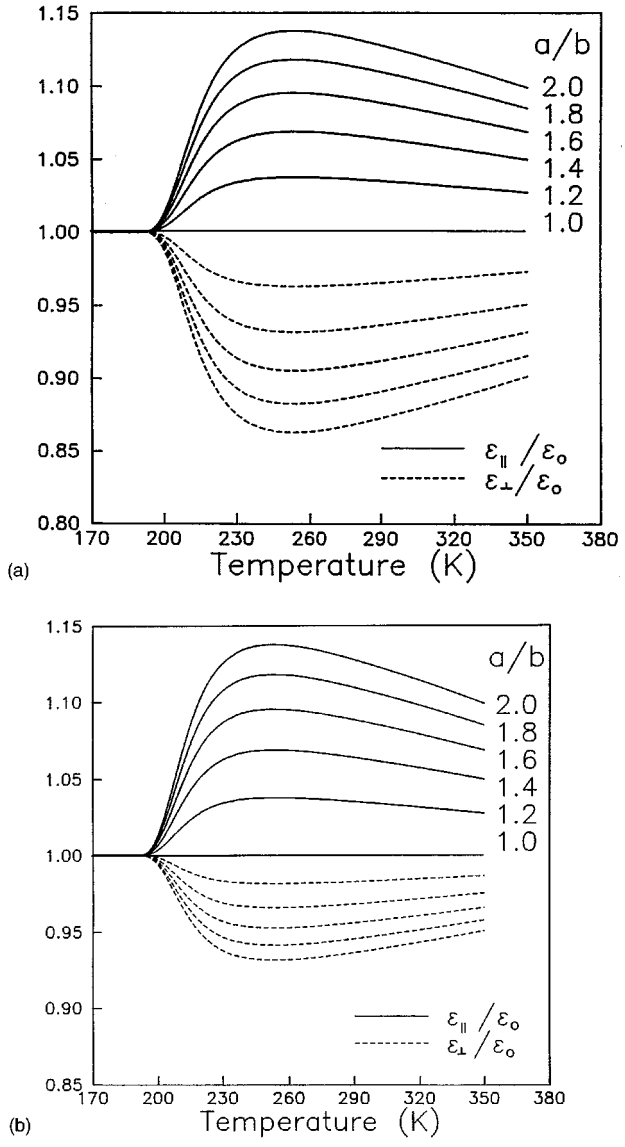

FIG. 8. The magnetodielectric anisotropy effect versus temperature for normal size distribution with different axial ratios; (a) for a 2D sample, (b) for a 3D sample.

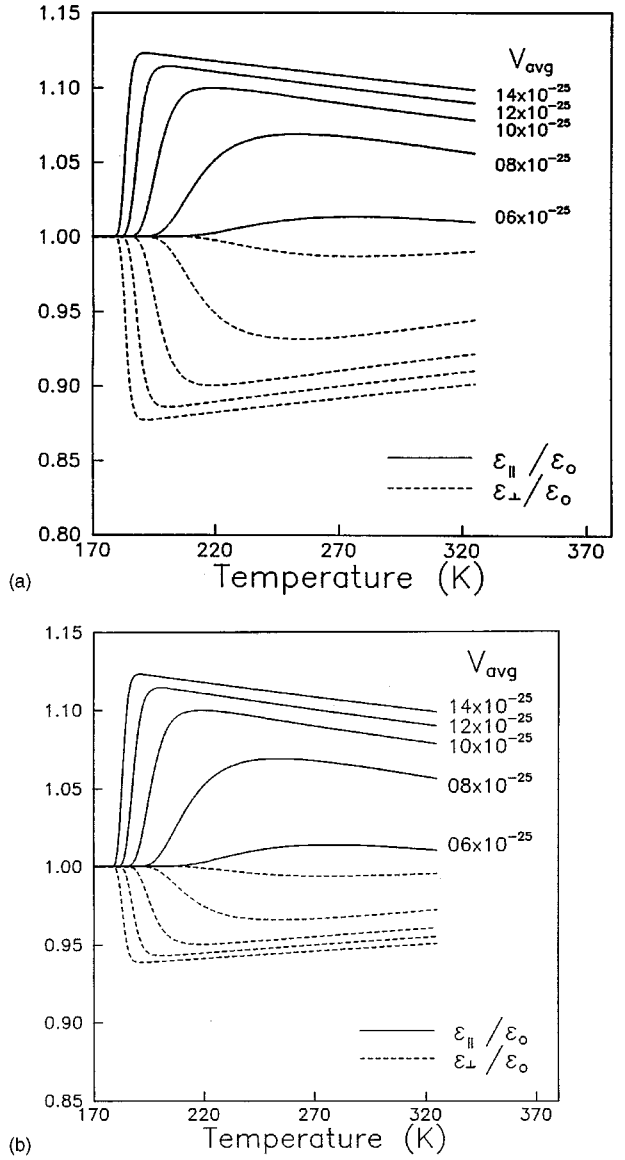

FIG. 9. The magnetodielectric anisotropy effect versus temperature for normal size distribution with different average volumes; (a) for a 2D sample, (b) for a 3D sample.

Fig. 1(b) are in good agreement with those reported by Mailfert and Nahounou,[6] Fannin, Scaife, and Charles,[8] and Chantrell.[10] Furthermore the increase of this effect for both the two- and three-dimensional systems with the axial ratio is in good agreement with the calculated results reported by Kopcansky *et al.*[4] It is important to note that the theoretical results reported by Chantrell[10] and Mailfert *et al.*[6] were based on a three-dimensional system. Since the applied magnetic field plays the role of an orienting agent of the particles and is the cause of the chain formation, in the absence of the field the average projection length of a particle in all directions is the same due to the random orientation of the particles in the fluid, consequently the magnetodielectric anisotropy effect is not expected to appear. However, when a magnetic field is applied the average projection length in the field direction becomes larger than that in directions normal to the field and mechanical anisotropy arises in the sample leading to the magnetodielectric anisotropy effect. It is worth mentioning that the average length in the field direction increases with the field, while the average length normal to the field direction decreases with the applied field. Therefore, the dielectric constant $\varepsilon_{\parallel}$ in the field direction increases, while $\varepsilon_{\perp}$ that is normal to the field direction decreases. Our calculated results in Figs. 1(a) and 1(b) show a behavior consistent with the above picture. Increasing the axial ratio leads to an increase in the mechanical anisotropy which in turns increases the magnetodielectric anisotropy effect. Again our results in Fig. 1 show a behavior consistent with this picture. Increasing the volume of the particles for a given axial ratio results in increasing the absolute difference between the major and minor axes. Consequently the mechanical anisotropy of the sample increases and hence the magnetodielectric anisotropy effect increases. This behavior is what is seen in our results presented in Fig. 3. The similarity of our calculated results of the magnetodielectric effect for the single, normal, and log-normal size distributions, versus field, presented in Fig. 3 may be attributed to the fact that the Shliomis volume at that

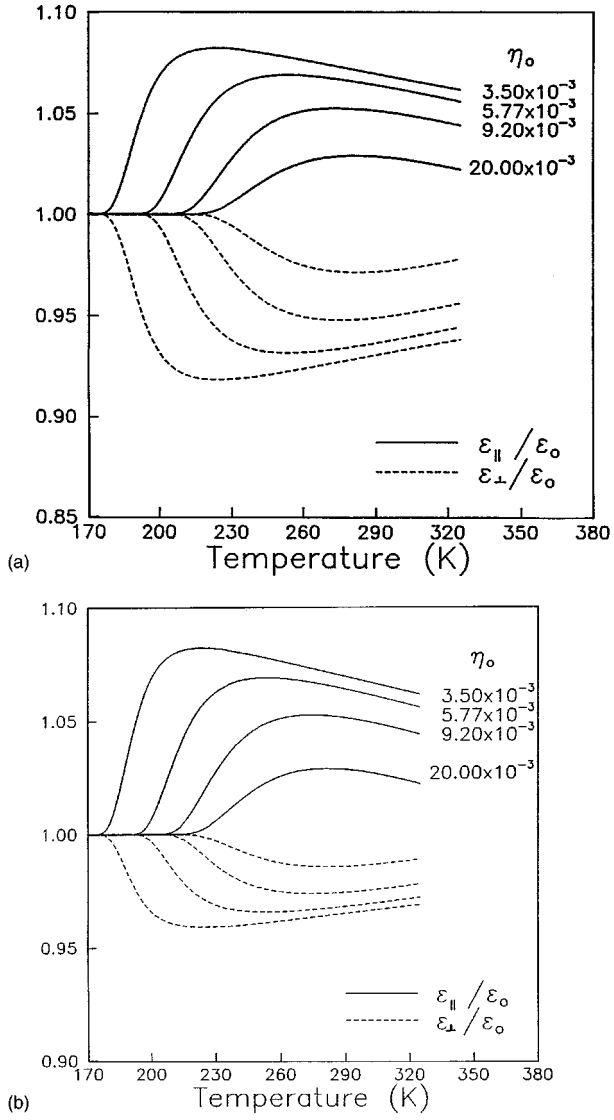

FIG. 10. The magnetodielectric anisotropy effect versus temperature for normal distribution and different carrier liquids; (a) for a 2D sample, (b) for a 3D sample.

temperature ($T=300$ K) is smaller than the average volume of the particles and therefore the majority of the particles orient themselves with the field.

The behavior of the magnetodielectric anisotropy effect with temperature presented in Figs. 5, 6, 7, 8, 9, and 10 are also explained in a similar way. Since the magnetodielectric anisotropy effect is a consequence of the field-induced mechanical anisotropy, only the unblocked (from physical rotation) particles with volumes $V>V_s$ that relax via the Brownian mechanism will contribute to the effect, while the blocked particles with $V<V_s$ that relax via the Néel mechanism will not contribute. Due to the presence of a particle size distribution, at any temperature there will be a portion of blocked particles and another portion of unblocked particles. Lowering the viscosity leads to a smaller Shliomis volume and consequently to a larger portion of unblocked particles and hence to a larger magnetodielectric anisotropy effect is. Increasing the temperature has two basic effects, firstly it decreases the viscosity and hence it increases the portion of unblocked particles; secondly it increases the thermal agitation which tends to randomize the orientation of the particles and to breakup the already existing chains. It is the balance between these two competing effects, i.e., the increase of the portion of unblocked particles and the thermal agitation, that determines the behavior of the magnetodielectric anisotropy effect in the magnetic fluids. At low temperatures, $T<T_s$, the Shliomis volume V_s is larger than the maximum volume and hence no particles will contribute to the magnetodielectric anisotropy effect. For temperatures $T>T_s$ the Shliomis volume V_s becomes smaller than $V_{\max}$ and a portion of the particles will contribute to the magnetodielectric anisotropy effect. At any temperature above T_s a portion of the particles with volumes smaller than V_s will be blocked from the physical rotation while those with $V>V_s$ will rotate physically and contribute to the magnetodielectric anisotropy effect. Further increase of temperature lowers V_s and thus increases the portion of unblocked particles leading to an increase in the magnetodielectric anisotropy effect. Although increasing the temperature increases the role of thermal agitation, which randomizes the orientation of the particles and tends to reduce the magnetodielectric anisotropy effect, it also results in a decrease in the viscosity and thus increases the number of unblocked particles. This increase in the number of unblocked particles overcomes the effect of thermal agitation leading to an increase of the magnetodielectric anisotropy. This process of converting blocked particles to unblocked particles continues and the magnetodielectric anisotropy continues to increase until a certain temperature T_m at which optimum conditions of orientation and chain formation occur. At this temperature the average projection length of the particles in the field direction is a maximum, while that in directions normal to the field is a minimum. Therefore one expects to have a maximum in $(\varepsilon_\parallel/\varepsilon_0)$ and a minimum in $(\varepsilon_\perp/\varepsilon_0)$.

For temperatures $T>T_m$, more particles are unblocked but at a low rate, and the role of thermal agitation still increases. In this range of temperature the role of thermal agitation as a randomizing effect dominates the low rate of converting blocked particles to unblocked ones. Therefore, the average projection length in the field direction decreases, while that in directions normal to to the field increases. Consequently $(\varepsilon_\parallel/\varepsilon_0)$ decreases while $(\varepsilon_\perp/\varepsilon_0)$ increases with increasing temperature in this range. At high enough temperatures, the majority of the particles are unblocked and the rate of conversion becomes very small, while thermal agitation still increases leading to further decrease in the magnetodielectric anisotropy effect until it becomes absent. The increase of the magnetodielectric effect from zero to a maximum in an abrupt way for the single volume is due to the fact that all the particles are converted from the blocked to the unblocked state in unison, while for the case of size distribution this conversion is gradual and therefore the rise to the maximum is gradual. A look at the results presented in Figs. 5, 6, and 7 shows a behavior consistent with this picture. It is worth mentioning that our results on the variation of $\varepsilon_\parallel$ and $\varepsilon_\perp$ with temperature are qualitatively similar to those reported by Derriche *et al.*,[1] and by Yusuf *et al.*[9] The role of viscosity on the magnetodielectric anisotropy effect is understood in terms of its effect on the Shliomis volume. The higher the viscosity, the larger the Shliomis volume, and consequently the lower the effect is and the higher the tem-

perature at which the maximum in $\varepsilon_{\parallel}/\varepsilon_0$ and the minimum in $\varepsilon_{\perp}/\varepsilon_0$ occurs is.

In all the calculations presented in this work, the magnetodielectric anisotropy factor $g(H,\omega)=1$ for the 2D sample and it is equal to 2 for the 3D sample. It is therefore suggested that dimensionality plays an important role in the magnetodielectric anisotropy effect in magnetic fluids; and it is crucial to consider the dimensionality of the samples when comparing results obtained by different workers in the field.

VI. CONCLUSION

The magnetodielectric anisotropy effect in magnetic fluids have been numerically calculated for monodispersed noninteracting particles for a 2D and 3D magnetic fluid. The calculations are based on the assumption that the dielectric constant at a given wavelength is proportional to the average projection length of the particles. In the calculation of the average projection length of the particles, the variation of viscosity with temperature, concentration, and applied magnetic field has been taken into consideration. Although interparticle interactions and field-induced chain formation have not been accounted for in the calculations, our results on the field dependence and the temperature variation of the magnetodielectric anisotropy effect are qualitatively in good agreement with previously reported theoretical and experimental results.

ACKNOWLEDGMENTS

We greatly appreciate the support provided by the Center for Theoretical and Applied Physics (CTAP) at Yarmouk University at which the calculations were carried out. S.M. would like to thank the (CTAP) for providing the financial support for his visit to Yarmouk University during which this work was accomplished.

[1] O. Derriche, L. Jorat, G. Noyel, and J. Monin, J. Magn. Magn. Mater. **102**, 155 (1991).
[2] A. Colteu, J. Magn. Magn. Mater. **39**, 88 (1983).
[3] A. Cotae, J. Magn. Magn. Mater. **39**, 85 (1983).
[4] P. Kopcansky, J. Cernak, P. Macko, D. Spisak, and K. Marton, J. Phys. D **22**, 1410 (1989).
[5] B. Z. Kaplan and D. M. Jacobson, Nature (London) **259**, 654 (1976).
[6] A. J. Mailfert and B. Nahounou, IEEE Trans. Magn. **16**, 254 (1980).
[7] A. Espurz, J. M. Alameda, and A. Espurz-Nieto, J. Phys. D **22**, 1174 (1989).
[8] P. C. Fannin, B. K. Scaife, and S. W. Charles, J. Magn. Magn. Mater. **122**, 168 (1993).
[9] N. A. Yusuf, J. Shobaki, H. Abu-Safia, and I. Abu-Aljarayesh, J. Magn. Magn. Mater. **149**, 373 (1995).
[10] R. W. Chantrell, J. Magn. Magn. Mater. **45**, 100 (1984).
[11] R. W. Chantrell, J. Popplewell, and S. W. Charles, IEEE Trans. Magn. **14**, 975 (1987).
[12] N. Y. Ayoub, A. Bradburay, R. W. Chantrell, and J. Popplewell, J. Magn. Magn. Mater. **65**, 185 (1987).
[13] M. I. Shliomis, Sov. Phys. Usp. **17**, 153 (1974).
[14] M. I. Shliomis, Sov. Phys. JETP **34**, 1291 (1972).
[15] U. Hartmann and H. H. Mende, J. Magn. Magn. Mater. **45**, 100 (1984).
[16] U. Hartmann and H. H. Mende, Phys. Status Solidi **82**, 481 (1984).
[17] P. C. Scholten, IEEE Trans. Magn. **16**, 221 (1980).
[18] P. C. Scholten, J. Magn. Magn. Mater. **39**, 99 (1983).
[19] J. P. McTague, J. Chem. Phys. **51**, 133 (1969).
[20] V. E. Fertman, *Magnetic fluids Guide book: Properties and Applications* (Hemisphere, New York, 1990).
[21] S. O. Gladkov, Physica B **160**, 211 (1989).
[22] M. I. Shliomis and V. I. Stepanov, J. Magn. Magn. Mater. **122**, 176 (1995).
[23] N. A. Yusuf, A. Ramadan, and H. Abu-Safia (unpublished).
[24] N. A. Yusuf, J. Shobaki, F. Rawwagah, and I. Abu-Aljarayesh, J. Magn. Magn. Mater. **149**, 373 (1995).